

Figure 5-3 displays the relationship between the measured and back-calculated concentration profiles during an *E. coli* RS2GFP tracer test on F1 at a specific discharge of 30 m/d. The upper and lower boundaries were measured with 95% confidence using t-statistics, such that $\mu \pm t \cdot \frac{s}{\sqrt{n}}$ represents the envelope in which the sample mean will fall 95% of the time. t is the level of significance of a two-tail test, s is the standard deviation of the acquired samples, and n is the number of samples counted per time interval. The degrees of freedom are $n-1$.

Figure 5-3 portrays the typical trends of *E. coli* RS2GFP transport observed at almost all specific discharges through both fracture samples. Effluent concentrations escalated rapidly near the beginning of each test, reached a peak, and then tailed off in a gradual manner, suggesting a non-Fickian transport behaviour. This is highly attributable to preferential flow paths, which rapidly transport a large portion of the mass. The remaining recovered mass, which is explained by the elongated tail of the effluent break-through curve, experienced a more tortuous flow path, encountering reduced velocity regions and a variety of obstacles along the way. All other breakthrough curves, including both measured and back-calculated concentrations, are presented in Appendix B. The data presented in the remainder of this chapter pertains to the back-calculated concentration profiles, unless stated otherwise.

Although most *E. coli* RS2GFP tracer tests exhibited a breakthrough curve consisting of early peaks and elongated tails, the amount of mass recovered from each test varied significantly. The amount of *E. coli* RS2GFP recovered was determined by integrating the back calculated effluent breakthrough curve, and compare the recovered mass to the mass that was initially

introduced to the flow field at the commencement of the test. Table 5-3 details the amount of *E. coli* RS2GFP recovered from each experiment.

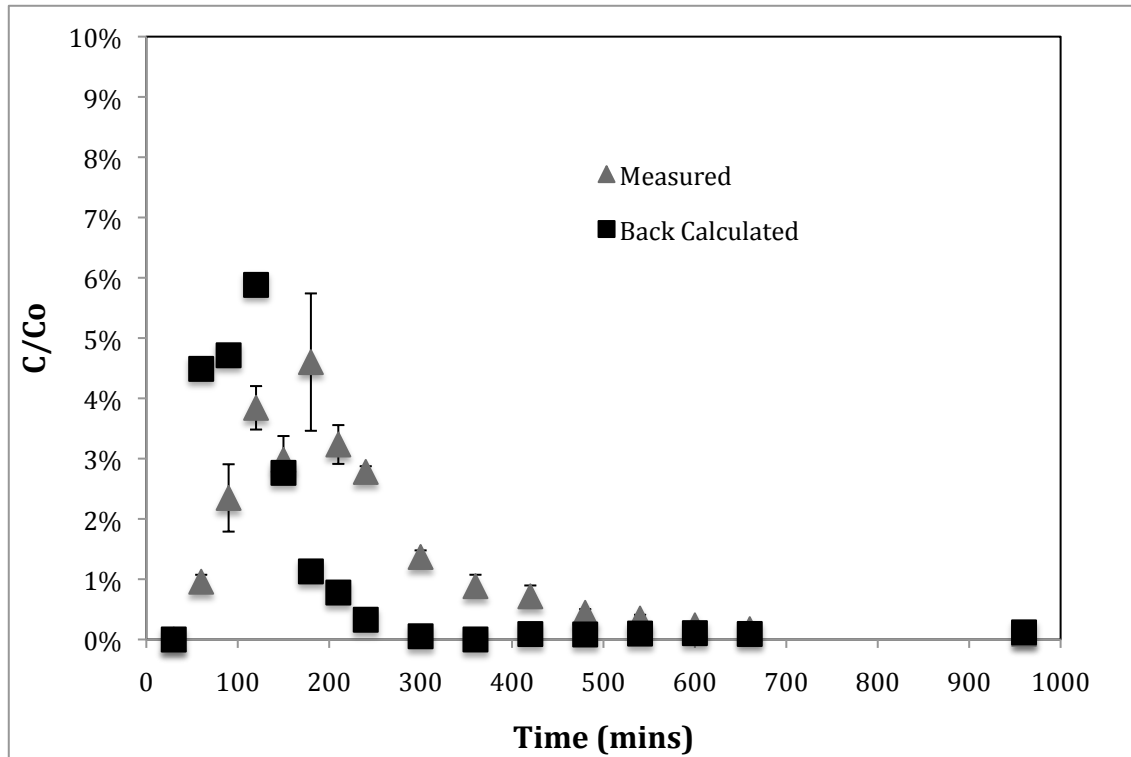


Figure 5-3: Measured vs back calculated breakthrough curves for F1 at a specific discharge of 30 m/day

From table 5-3 it is apparent that, on average, F1 retained significantly more mass than F2 in all experiments. This is of interest as the both the aperture field variability (as shown in Table 5-2), and the mean hydraulic aperture are very similar for both fracture samples.

The aperture field variability was calculated as follows:

$$COV = \frac{\sigma_{b_h, b_f, b_m}}{b_m} \quad (18)$$

Mechanisms causing retention are discussed later on in this section.

Table 5-3: Percent recovery of *E. coli RS-2GFP*

Fracture ID	Specific Discharge [m/day]	Percent Recovery [%]	Mean Residence Time [min]
F1	30	14.63	148.64
	30	6.70	130.00*
	10	35.71	390.79
	5	6.23	650.00*
F2	30	62.17	177.43
	30	51.18	110.00*
	10	49.20	281.00
	5	9.64	500.00*

* manually calculated based on peak time of effluent concentration profile due to limitations of integration techniques

For F2, the recovery of mass displays a very straightforward trend. That is, as specific discharge decreases, so does mass recovery. However, F1 does not display this phenomenon. A specific discharge of 10 m/day seems to be a critical point at which *E. coli RS2GFP* transport is most facilitated (i.e it experiences the least retention). Differences in the relationship between specific discharge and percent recovery can be attributed to the fact that different transport

mechanisms are dominating within each fracture sample. Theoretically, increased specific discharge: (1) provides less of an opportunity for *E. coli* RS2GFP to attach to the fracture wall, as inertial forces significantly exceed attractive forces between the *E. coli* RS2GFP, and mean residence times are relatively short (refer to Table 5-4); and (2) introduces larger shear forces, thus increasing the likelihood of detachment. In essence, it was expected that increased specific discharges would lead to a higher recovery of mass and a shorter mean residence time.

Explaining why a specific discharge of 10 m/day in F1 resulted in a mass recovery that virtually doubled that found at 30 m/day involves a deeper look into the retention mechanisms that are at play. Indeed, specific discharge has a significant impact on retention, but evidently there are additional factors affecting retention within F1 that, when evaluated in conjunction with specific discharge, are just as, if not more important than specific discharge. In an ideal fracture plane consisting of two parallel plates, it would always be true that larger specific discharges lead to larger recoveries, as variability within the aperture field is non-existent. However, F1, being a natural fracture plane, hosts a highly variable aperture field which in some form contributed to the retention at a specific discharge of 30 m/day than at 10 m/day. In beginning to explain this, it is important to note that higher discharges allow biocolloids to sample a larger areal extent fracture plane, both in the y and z-directions. In other words, biocolloids are primarily and almost only transported along preferential pathways made up of interconnected large aperture regions at low specific discharges. At higher specific discharges, however, preferential flow paths expand as the critical pore entry pressures of smaller aperture regions increasingly become satisfied, and biocolloids then deviate from the primary preferential flow paths. This allows more opportunities

for transverse dispersion and therefore more opportunities to sample the entire fracture plane. Experiencing larger portions of the fracture plane equates to: (1) increased exposure to the matrix, thus providing a greater chance of attachment onto the matrix, (2) increased colloidal transport in smaller aperture regions, thus enhancing the opportunity for colloids to migrate to the fracture wall, and (3) more of an opportunity for *E. coli* RS2GFP to become lodged in the pore throats of small aperture regions (straining). Combined, these mechanisms have likely contributed to the enhancement of bacterial retention in F1 at a specific discharge of 30 m/day. Based on this phenomenon, it is also likely that there is a difference in the spatial distribution of flow paths present at relatively high specific discharges versus lower specific discharges.

A second reason that may have contributed to the difference in transport patterns found in F1 and F2 ties into the fact that fluid flow becomes far more complex as specific discharge increases. With the fluid moving three times faster at 30 m/day than at 10 m/day, it is likely that the flow lines stacked along the z-direction begin to deviate from being smooth and parallel (i.e. transitional and turbulent flow). As asperities and small aperture regions are encountered, flow lines are perturbed, providing *E. coli* RS2GFP with more of an opportunity to wander from the center of the aperture towards the regions near the fracture walls. That is, if the system were modeled, the movement of biocolloids from one flow line to the next would no longer be defined by a “random walk tracking method”, but would become biased by regions that are relatively rough. Once again, this phenomenon provides a greater opportunity for *E. coli* RS2GFP to come in contact with, and attach onto the fracture wall.

Figure 5-4 shows that a constant specific discharge resulted in similar shaped effluent concentration profiles for both F1 and F2. Both profiles display non-Fickian transport, suggesting a relatively high variability within each aperture field. However, the magnitude of the peaks found in each concentration profile varies significantly, suggesting once again that specific discharge, although it influences characteristics such as residence time, is not the dominant mechanism governing recovery in these experiments.

It is important to note that working with bacteria as a tracer is likely to induce more error than working with the solute and microsphere tracers. Issues such as survival, sample preparation and enumeration all contribute to the measure of error, in addition to error sources that also apply to solutes and microspheres employed in these experiments.

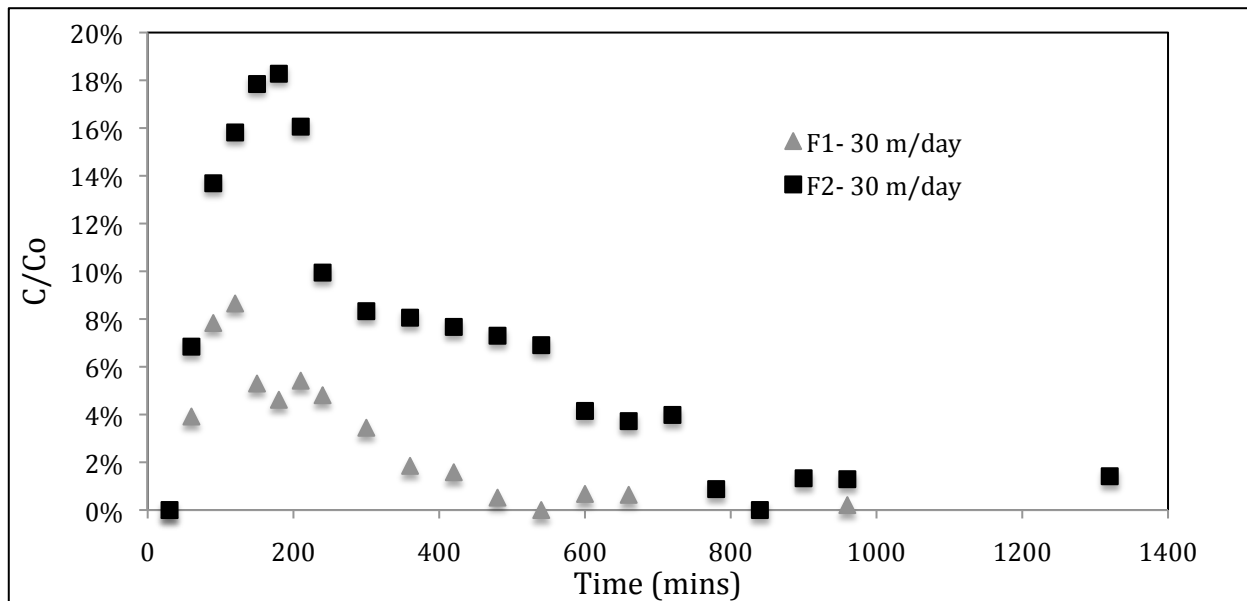


Figure 5-4: *E. coli* RS-2GFP breakthrough curves at a specific discharge of 30 m/day

5.1.4 Microsphere Tracer Tests

Applying the same methods and specific discharges used for the bromide and *E. coli* RS2GFP tracer tests, the transport and retention of microspheres was determined. Once again, it was important to differentiate between the measured calculation of microspheres in the effluent and the actual concentration that exited the fracture plane. This was accounted for using Equation 17.

The trends observed in Figure 5-5, which compares the measured and back calculated effluent concentration profiles of the microspheres in F1 at a specific discharge of 30 m/d, are very similar to those observed in the breakthrough curves of the bromide and *E. coli* RS2GFP tests. The effluent concentration rapidly reached a peak, and then experienced an elongated tail due to interactions with the matrix and a highly variable aperture field that induced a tortuous pathway for the remaining mass. Like the *E. coli* RS2GFP breakthrough curves, each microsphere tracer experiment generated effluent concentration profiles that were similar in shape to that of Figure 5-5. The effluent concentration profiles from the remaining microsphere experiments in both fractures are presented in Appendix C.

The microsphere tracer tests produced very consistent results. In those tests with a lower specific discharge, and thus a higher residence time, colloid recovery was relatively low. In other words, filtration mechanisms were more effective, as a whole, as specific discharge decreased. It is highly unlikely that filtration was due to straining because an aperture region small enough to filter out a particle that is only 0.05 μm would be infrequently encountered along the flow

pathways in a fracture plane with a equivalent hydraulic aperture greater than 100 μm . Additionally, the colloids were most likely transported through aperture regions that were much larger than their diameter. According to O'Melia (1980), for given surface and particle to come in

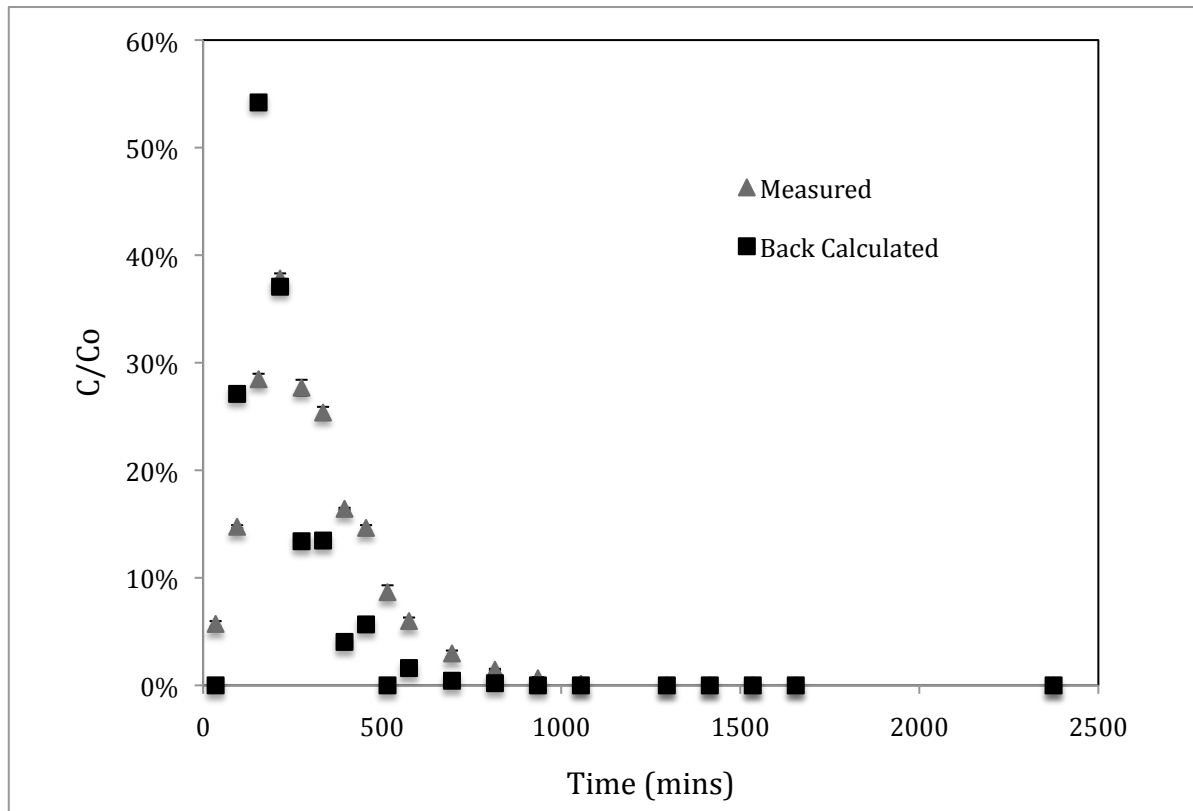


Figure 5-5: Measured and back-calculated effluent concentration profiles for F1 ($q = 30 \text{ m/day}$)

contact one of the following must occur: (1) interception of the particle trajectory, (2) gravitational settling, or (3) diffusion. Although possible, interception of the particle trajectory was likely minimal, as most flow regimes employed in this research induce flow lines parallel to

the fracture wall. However, at lower specific discharges, both diffusion and gravitational settling naturally become more influential.

The length scale of Stokes settling of a spherical particle, as previously discussed in Section 2.4.1, is defined as follows:

$$L_s = \left(\frac{1}{18\mu} \right) (\rho_p - \rho_f) g d^2 \Delta t$$

where, d [L] is the diameter of the particle, ρ_p [M/L³] is the density of the particle, ρ_f [M/L³] is the density of the fluid, μ [M/ LT] is the dynamic viscosity of the fluid, g [T/L²] is acceleration due to gravity and Δt [T] is the time interval. Settling only becomes important when the lower surface of the fracture wall can be reached during the time interval defined by Δt . When this measure is applied to a 0.05 μm microsphere (with a density of 1.05 g/mL), settling would take on average 23 days to occur in F1, and approximately 18 days to occur in F2. These times significantly exceed the duration of the tracer tests in which case settling can be deemed an insignificant retention mechanism. However, it is possible that some microspheres aggregated, forming a much larger unit, in which case settling may have been more prominent. The degree of aggregation that occurred during the colloid tracer tests remains somewhat ambiguous, and therefore direct conclusions about the magnitude of settling cannot be made.

Diffusion, however, is undeniably the most important factor with regards to the retention of microspheres. The influence of diffusion is inversely proportional to specific discharge, which explains why a higher degree of retention was attained at lower specific discharges. At low

specific discharges, microspheres were provided more of an opportunity to migrate to the fracture wall. Once at the fracture wall, microspheres could either attach to the wall, or continue to migrate into the matrix, at which point they would enter a stagnant flow regime. On a short time scale, diffusion into the matrix remains an irreversible process until the flow regime changes, meaning that microspheres migrating into the matrix remained there for the duration of the experiment. Additionally, low specific discharges allowed microspheres ample time to migrate into immobile aperture regions.

5.2 Comparing Solute, Biocolloid, and Colloid Tracer Tests

A thorough comparison of the three tracer tests applied in this research must be conducted to isolate hydrodynamic effects on particle transport. Prior to delineating hydrodynamic effects, it is important to extract the primary differences in transport between bromide, *E. coli* RS2GFP, and CMP microspheres. Bromide, being a conservative tracer, is strongly influenced by the physical properties of the fracture plane. A bromide ion is significantly smaller than both *E. coli* RS2GFP and the microspheres, and therefore effects such as size exclusion, straining and settling were negligible. *E. coli* RS2GFP, on the contrary, is highly influenced by both the surface properties of the fracture sample, as well as the physical properties of the aperture. During an experiment, *E. coli* RS-2GFP can: (1) experience growth and/or dieoff, (2) experience attachment to or repulsion from the fracture wall, (3) accumulate in small aperture regions where straining occurs, and (4) aggregate to form a larger unit. The transport of microspheres, like bromide, is influenced by the physical properties of the fracture plane, but because they possess a finite

diameter, they may be subject to mechanisms such as straining, settling and size exclusion. Additionally, microspheres can experience attraction to or repulsion from the fracture wall. All of these differences must be accounted for when comparing and contrasting the effluent concentration profiles of each of the tracer types.

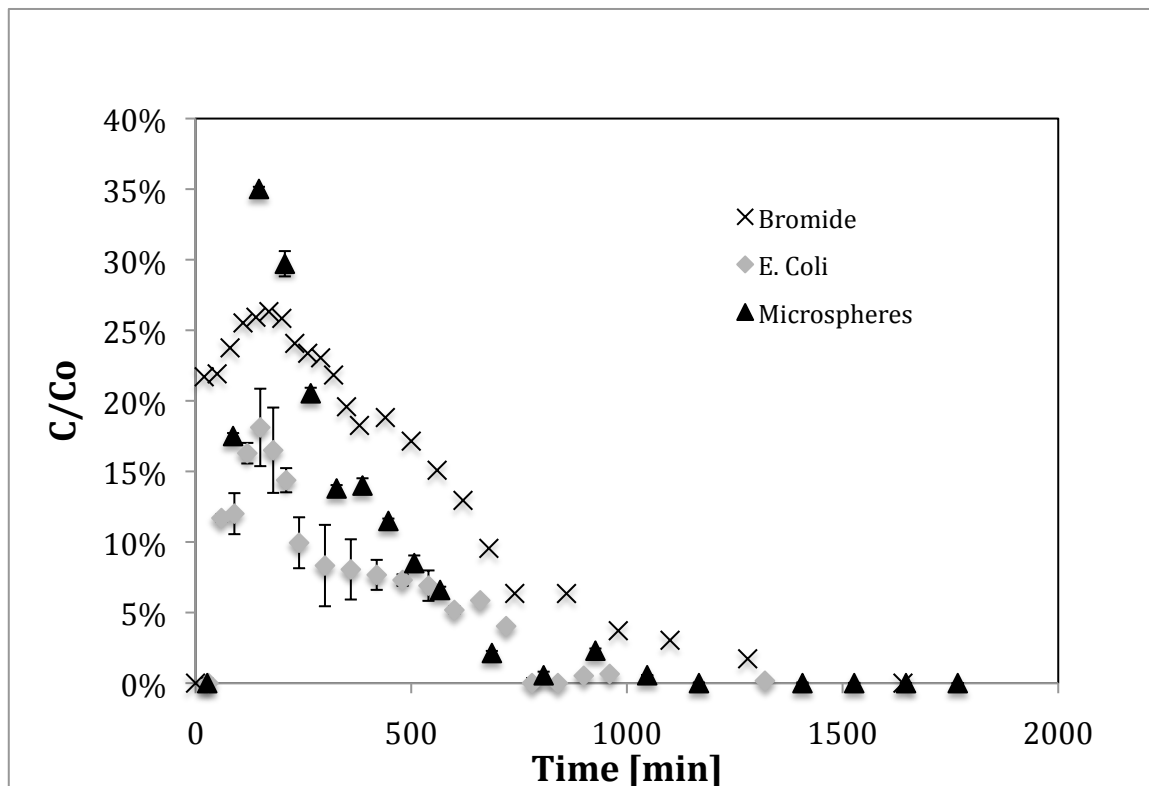


Figure 5-6: Differential transport by comparison of effluent concentration profiles for F2 ($q=30$ m/day)

The primary intent of using bromide, *E. coli* RS2GFP and polystyrene microspheres, was to evaluate the effects of particle size on transport. *E. coli* RS2GFP is considerably larger in size than the microspheres employed in these experiments, while the microspheres are significantly

larger in size than a bromide ion. Comparing and contrasting the resulting breakthrough curves of each tracer at a given specific discharge permits, to an extent, a means of isolating the influence of hydrodynamics on particle transport. These comparisons can be found in Figure 5-6. Interestingly, when examining Figure 5-6, it is noticeable that the peak concentration of each tracer eluted at the same time, a phenomenon that is highly supportive of the existence of preferential flow paths. To some degree, each tracer traveled along the same preferential flow path as the next, permitting early arrival times and thus resulting in similar peaks. However, the magnitude of each peak differed significantly. As expected, *E. coli* RS2GFP, being the most sizeable tracer, experienced the smallest peak. This can be explained by the various retention mechanisms discussed in section 5.1.3. Bromide experienced a peak larger than that of *E. coli* RS-2GFP but somewhat smaller than the peak found in the microsphere effluent concentration profile. Additionally, the bromide tracer experienced the most tortuous transport pathway, which explains the elongated tail of the bromide effluent concentration profile. This is likely attributable to frequent interactions with both the matrix and immobile aperture regions. Comparing recovery of the three tracers also gives hints as to how hydrodynamics affect particle transport. Figure 5-7 shows that percent recovery in all instances was ordered as follows: $\text{Br}^- > \text{CMP microspheres} > E. coli \text{ RS2GFP}$, proving that particle size influences transport within all flow regimes.

It is noticeable from all the experiments conducted in this research, that *E. coli* consistently experienced greater retention than both bromide and the microspheres. Additionally, the relationship between mass recovery and specific discharge was found to be different for *E. coli* than it was for bromide and the microspheres. Classically, it can be expected that increased

specific discharge results in increased recovery, as particles are given less time to attach or settle, and increased shear forces encourage the detachment of attached particles. This phenomenon was exhibited in the bromide and microsphere tracer tests, but not in the *E. coli* tracer tests. *E. coli*, in F1 experienced greater retention at a specific discharge of 30 m/d than it did at 10 m/d, and experienced the same amount of retention at both 10 and 30 m/d in F2. This can be explained by the influence of hydrodynamics on particle transport. As specific discharge increases, hydrodynamic forces increasingly help larger particles overcome the energy barrier (i.e. electrostatic repulsion) between the particle and the fracture wall. Overcoming this barrier allows particles to enter into a region where collision with and attachment to the fracture wall is permitted. Hydrodynamic forces, however, have very little impact on the transport of smaller particles such as the microspheres employed in this research. This phenomenon was far more prominent in F1 as F2 did not capture the critical specific discharge at which local turbulences come into effect.

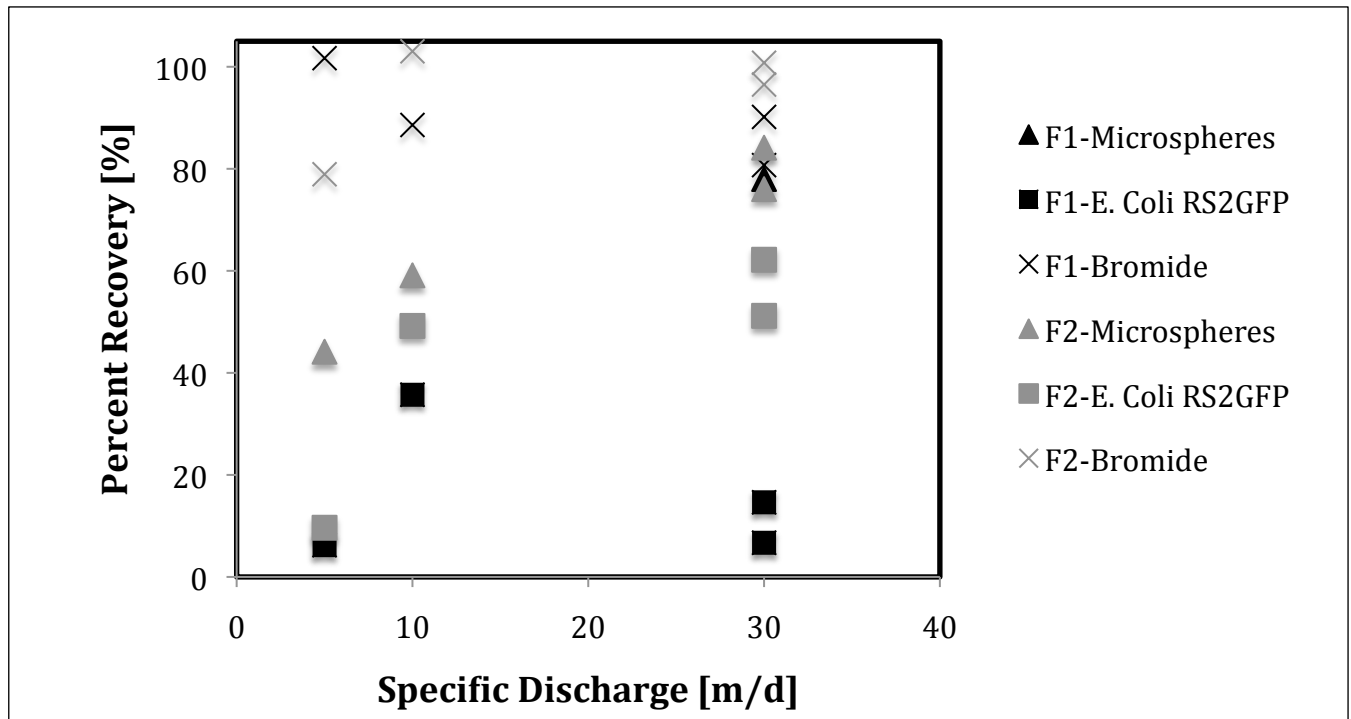


Figure 5-7: Comparison of recovery

6. Conclusions and Future Recommendations

Research involving experiments on different aperture fields, at differing specific discharges, using different sized colloids suggests the following details regarding the influence of hydrodynamics on colloid transport:

- Hydraulic tests revealed a linear relationship between the hydraulic head gradient across the flow field and specific discharge. Linearity suggests a laminar flow regime, thus validating the application of the cubic law to define the hydraulic aperture, b_h .
- Based on their effluent concentration profiles, solutes, colloids, and biocolloids are transported in a non-Fickian manner through saturated fractured media at all specific discharges. Non-Fickian transport supports the idea that there is not a constant centre of mass throughout the duration of a tracer test.
- Both solutes and colloids (including biocolloids) were transported along preferential flow paths, which covered a larger aerial extent of the fracture as specific discharge increased.
- Based on the mean residence time of bromide in the solute tracer tests, and the drastic difference in the recovery of the biocolloids in F1 compared to F2 (at each specific discharge percent recovery of biocolloids in $F2 > F1$) it is likely that F1 hosted more tortuous flow paths.

- Transport rates, based on the duration of the tracer tests, were ordered as follows *E. coli* RS2GFP > CMP microspheres > bromide. This is attributable to the ease at which solutes and smaller colloids diffuse from the centerline of the flow channel into the immobile regions adjacent to the fracture wall and/or the matrix (i.e solutes, and to some extent small colloids follow Taylor dispersion; they sample the entire flow field in the y-direction). Additionally, solutes and small colloids were able to sample a larger aerial extent of the fracture plane due to their higher coefficients of diffusion.
- For small colloids and solutes, mass recovery increased with increasing specific discharge. For the larger colloids, which in this research are *E. coli* RS2GFP, there is not always a linear relationship between specific discharge and mass recovery. For highly variable aperture fields, there appears to be a critical point at which specific discharge is not quite high enough for hydrodynamic forces to significantly exceed the energy barrier between the biocolloid and the fracture wall, and remains slow enough so that the preferential flow paths only sample a small portion of the fracture plane (only large aperture regions), thus limiting the impact of both straining and attachment.
- In laminar flow regimes, flow rate is most influential on the transport of solutes and small particles where effects such as straining and settling are virtually negligible.
- The transport of larger particles, such as *E.coli*, is highly governed by hydrodynamics, which plays an important role in the coupling of factors such as size and charge exclusion, and settling. The hydrodynamics forces present at relatively high specific discharges (i.e 30 m/day) allow larger particles to overcome the energy barrier (i.e electrostatic

repulsion) between the particles and the fracture wall. This permits the first step of attachment, in which the particle is permitted to collide with the fracture wall. Overall, increasing hydrodynamic forces allow higher degrees of attachment, and thus promote a decrease in mass recovery.

- Hydrodynamic forces do not affect particles smaller than $\sim 1\mu\text{m}$ in size (e.g. microspheres), making it difficult for these particles to overcome the energy barrier required to come in contact with the fracture wall. Less interaction with the fracture wall limits attachment, and leads to higher particle recoveries.
- Specific discharge becomes increasingly important at higher specific discharges for all particle sizes, as high flow velocities promote detachment, and limit the amount of time available for diffusion, attachment and settling to occur.
- Interaction with the fracture matrix as well as stagnant flow regimes becomes increasingly important with smaller colloids, as their increased diffusivities promote migration into these zones. Specific discharge dictates the degree of interaction with the matrix and stagnant aperture regions, as high average flow velocities limit the amount of time that colloids can diffuse into these regions. This phenomenon is supported by the microsphere tracer tests, during which decreased specific discharges lead to increased retention. Retention of microspheres was primarily attributed to diffusion into immobile aperture regions as well as the matrix.
- In general, all experiments conducted in this research prove that there is a potential for the rapid transport of colloidal contaminants within fracture environments, including

pathogenic microorganisms and radionuclides. It is likely that because of their widespread presence, these contaminants are seeping into fractured systems from sewage lines, septic beds, and landfills, and are gradually degrading the quality of water in surrounding aquifers.

Recommendations and Limitations

- Evaluate the transport of a colloid containing a diameter greater than $0.05\mu\text{m}$, yet smaller in size than *E. coli* RS2GFP, to determine whether there is an optimum particle diameter that is primarily influenced by hydrodynamics, and not as bogged down by the influences of diffusion, as was the case for the microspheres, or settling, straining, and attachment, as experienced by the *E. coli* RS2GFP.
- In order for the results presented in this research to be translatable to the field, it would be ideal to mimic field conditions such as water temperature and water chemistry.
- Comparing the transport of a colloid that is rod-shaped with a soft cell wall and local charges, to that of a hard surfaced, spherical particle with a uniform charge does not minimize the variables involved in isolating hydrodynamic influence on particle transport. To truly evaluate the impact of hydrodynamics, one would have to make use of particles (i.e microspheres) that only differ in size, but hold roughly the same charge and shape, thus making particle size the only variable within a given experiment.

- To expand upon this research, it would be valuable to apply the exact experiments executed in this research to different rock types. This would help determine whether the concepts derived from this research can be universally applied to multiple rock types or whether it is limited to dolomitic limestone.
- A possible experimental improvement would be to use pulsation-free pumps to pump water through the fracture plane to simulate flow within the natural environment. Although it likely wasn't significant, pulsing flow may have had an influence on attachment, as pulses would perturb attached colloids.

References

- Ahmadi, G. (2009). Transport, Deposition and Removal of Charged Nano-Particles. *RTO-EN-AVT-169 - Modeling and Computation of Nanoparticles in Fluid Flows*. North Atlantic Treaty Organization.
- Auradou, H. (2009). Influence of wall roughness on the geometrical, mechanical and transport properties of single fractures. *Journal of Physics D: Applied Physics*, 42(21), 1-10. doi:10.1088/0022-3727/42/21/214015
- Auradou, H, Drazer, G., Boschan, A., Hulin, J. P., & Koplik, J. (2006). Flow channeling in a single fracture induced by shear displacement. *Geothermics*, 35(5-6), 576-588.
- Batchelor, G. K. (1967). *An Introduction to Fluid Dynamics*. Cambridge: Cambridge University Press.
- Becker, M. W. (2004). Distinguishing Advection, Dispersion, and Diffusion in Fractured Bedrock. *2004 U.S. EPA/NGWA Fractured Rock Conference: State of the Science and Measuring Success in Remediation* (pp. 685-693). Portland, Maine.
- Becker, M. W., Metge, D. W., Collins, S. A., Shapiro, A. M., & Harvey, R. W. (2003). Bacterial Transport Experiments in Fractured Crystalline Bedrock. *Groundwater*, 41(5), 682-689.
- Becker, M. W., Reimus, P. W., & Vilks, P. (1998). Transport and Attenuation of Carboxylate-Modified Latex Microspheres in Fractured Rock Laboratory and Field Tracer Tests. *Groundwater*, 37(3), 387-395.
- Becker, W., & Shapiro, A. M. (2000). Tracer transport in fractured crystalline rock : Evidence of nondiffusive breakthrough tailing. *Water Resources*, 36(7), 1677-1686.
- Berger, P. (2008). Viruses in Ground Water. *Dangerous Pollutants (Xenobiotics) in Urban Water Cycle*, 131-149.
- Bergey, D. H., Holt, J. G., & Krieg, N. R. (1984). *Bergey's Manual of Systematic Bacteriology*. Baltimore: Williams & Wilkins.
- Berkowitz, B. (2002). Characterizing flow and transport in fractured geological media: A review. *Advances in Water Resources*, 25(8-12), 861-884. doi:10.1016/S0309-1708(02)00042-8
- Bodin, J., Delay, F., & de Marsily, G. (2003). Solute transport in a single fracture with negligible matrix permeability: 1. Fundamental mechanisms. *Hydrogeology Journal*, 11(4), 418-433. doi:10.1007/s10040-003-0268-2
- Borchardt, M. A., Bradbury, K. R., Gotkowitz, M. B., Cherry, J. A., & Parker, B. L. (2007). Human Enteric Viruses in Groundwater from a Confined Bedrock Aquifer Human Enteric Viruses in Groundwater from a Confined Bedrock Aquifer. *Environmental Science & Technology*, 41(August), 6606-6612. doi:10.1021/es071110
- Briggs, S. A., Sleep, B. E., & Karney, B. W. (2009). Modeling of rock fracture flow using the Lattice Boltzmann Method on graphics hardware. *Rock Mechanics*, 2009(May), 1-10.

- Brown, R. S., & Hussain, M. (2003). The Walkerton tragedy—issues for water quality monitoring. *The Analyst*, 128(4), 320-322. doi:10.1039/b301945b
- Brush, D. J., & Thomson, N. (2003). Three-Dimensional Fluid Flow and Solute Transport in Rough-Walled Fractures. *Water Resources Research*, 39(4), 1085. doi:10.1029/2002WR001346
- Canadian Ground Water Association (2010). Groundwater. Retrieved March 2011, from <http://www.cgwa.org/education.htm>
- Celico, F., Varcamonti, M., Guida, M., & Naclerio, G. (2004). Influence of Precipitation and Soil on Transport of Fecal Enterococci in Fractured Limestone Aquifers. *Applied and Environmental Microbiology*, 70(5), 2843-2847. doi:10.1128/AEM.70.5.2843
- Cumbie, D. H., & McKay, L. D. (1999). Influence of diameter on particle transport in a fractured shale saprolite. *Journal of Contaminant Hydrology*, 37(1-2), 139-157. doi:10.1016/S0169-7722(98)00156-9
- Degueldre, C., Baeyens, B., Goerlich, W., Riga, J., Verbist, J., & Stadelmann, P. (1989). Colloids in water from a subsurface fracture in granitic rock, Grimsel Test Site, Switzerland, *Geochimica et Cosmochimica Acta*, 53(3), 603-10.
- de Kerchove, A. J., & Elimelech, M. (2005). Relevance of Electrokinetic Theory for “Soft” Particles to Bacterial Cells: Implications for Bacterial Adhesion. *Langmuir*, 21(14), 6462-6472. doi:10.1021/la047049t
- Dickson, S. E., & Thomson, N. (2003). Dissolution of entrapped DNAPLs in variable aperture fractures: Experiments and empirical model development. *Environmental Science & Technology*, 37, 4128-4137.
- Dijk, P., Berkowitz, B., & Bendel, P. (1999). Investigation of flow in water-saturated rock fractures using nuclear magnetic resonance imaging (NMRI). *Water Resources Research*, 35(2), 347-360.
- Dowd, S. E., Pillai, S. D., Wang, S. Y., & Corapcioglu, M. Y. (1998). Delineating the specific influence of virus isoelectric point and size on virus adsorption and transport through sandy soils. *Applied and Environmental Microbiology*, 64, 405-410.
- Durham, W. B., & Bonner, B. P. (1994). Self-propping and fluid flow in slightly offset joints at high effective pressures. *Journal of Geophysical Research*, 99, 9391–9399.
- Emelko, M. B., Schmidt, P. J., & Roberson, A. (2008). Quantification of uncertainty in microbial data – reporting and regulatory implications. *Journal of American Water Works Association*, 100(3), 9-19.
- Fahim, M. A., & Wakao, N. (1982). Parameter Estimation from Tracer Response Measurements, *The Chemical Engineering Journal*, 25, 1 - 8.
- Fetter, C., (1999). *Contaminant Hydrogeology*. (A. McConnin, Robert, Ed.) (2nd ed.). Upper Saddle River, New Jersey: Prentice-Hall, Inc.

- Fontes, D. E., Mills, a L., Hornberger, G. M., & Herman, J. S. (1991). Physical and chemical factors influencing transport of microorganisms through porous media. *Applied and Environmental Microbiology*, 57(9), 2473-2481.
- Foppen, J. W., & Schijven, J. F. (2006). Evaluation of data from the literature on the transport and survival of Escherichia coli and thermotolerant coliforms in aquifers under saturated conditions. *Water research*, 40(3), 401-426. doi:10.1016/j.watres.2005.11.018
- Gale, J., MacLeod, R., & LeMessurier, E. (1990). Site characterization and validation - Measurement of flow rate, solute velocities and aperture variation in natural fractures as a function of normal and shear stress, stage 3, *Stripa Project Report 90-11*, Swedish Nuclear Fuel and Waste Management Company, Stockholm
- Garnier, J. (1985). Retardation of dissolved radiocarbon through a carbonate matrix. *Geochemica et Cosmochimica Acta*, 49(3), 683-693.
- Gilbert, P., Evans, D. J., Evans, E., Duguid, I. G., & Brown, M. R. (1991). Surface characteristics and adhesion of Escherichia coli and Staphylococcus epidermidis. *The Journal of Applied Bacteriology*, 71(1), 72-7.
- Glennon, R. J. (2002). *Water Follies: Groundwater Pumping and the Fate of America's Fresh Waters* (p. 2). Washington, D.C: Island Press.
- Gvirtzman, H., & Gorelick, S. M. (1991). Dispersion and advection in unsaturated porous media enhanced by anion exclusion. *Nature*, 352, 793-795.
- Happel, J., & Brenner, H. (1965). *Low Reynolds number hydrodynamics: With special applications to particulate media*. Englewood Cliffs, NJ: Prentice-Hall Inc.
- Harvey, R. W., George, L. H., Smith, R. L., & Leblanc, D. R. (1989). Microspheres and Indigenous Bacteria through a Sandy Aquifer: Results of Natural- and Forced-Gradient Tracer Experiments. *Society*, 23(1), 51-56.
- Iwai, K. (1976). *Fundamental studies of the fluid flow through a single fracture*. Ph.D Thesis. University of California, Berkeley.
- Jin, Y., Chu, Y., & Li, Y. (2000). Virus removal and transport in saturated and unsaturated sand columns. *Journal of Contaminant Hydrology*, 111-128.
- John, David, E., & Rose, J. B. (2005). Critical Review of Factors Affecting Microbial Survival in Groundwater. *Environmental Science & Technology*, 39(19), 7345-7356.
- Keller, A., Roberts, P. V., & Kitanidis, P. K. (1995). Prediction of single phase transport parameters in a variable aperture fracture. *Geophysical Research Letters*, 22(11), 1425-1428.
- Koyama, T., Neretnieks, I., & Jing, L. (2008). A numerical study on differences in using Navier–Stokes and Reynolds equations for modeling the fluid flow and particle transport in single rock fractures with shear. *International Journal of Rock Mechanics and Mining Sciences*, 45(7), 1082-1101. doi:10.1016/j.ijrmms.2007.11.006

- Lomize, G. M. (1951). Flow in Fractured Rocks. Moscow: Gosenergoizdat
- Louis, C. (1969). A Study of Groundwater Flow in Jointed Rock and its Influence on the Stability of Rock Masses (p. 90). Imperial College Rock Mechanics Research Report.
- Macler, B. A., & Merkle, J. C. (2000). Current knowledge on groundwater microbial pathogens and their control. *Hydrogeology Journal*, 8(1), 29-40. doi:10.1007/PL00010972
- Malard, F., Reygrobelle, J., & Soulie, M. (1994). Transport and retention of fecal bacteria at sewage-polluted fractured rock sites. *Journal of Environmental Quality*, 23(6), 1352-1363.
- McDowell-Boyer, L. M., Hunt, J. R., & Sitar, N. (1986). Particle Transport Through Porous Media. *Water Resources Research*, 22(13), 1901-1921.
- McKay, L. D., Sanford, W., & Strong, J. M. (2000). Field-scale migration of colloidal tracers in a fractured shale saprolite. *Ground Water*, 38(1), 139-147.
- Motter, K., & Jones, C. (2008). Standard Operating Procedure for the Analysis of Chloride , Bromide and Sulfate in Fresh Waters by Ion Chromatography. *Public Health*. Corvallis.
- Mourzenko, V. V., Thovert, T., & Adler, P. M. (1995). Permeability of a single fracture: validity of the Reynolds equation. *Journal de Physique II*, 5, 465-482.
- Natural Resources Canada (2005), How well do we understand Groundwater in Canada? A science case study, ESS no. 2005030, 41pp
- Neuman, S. P. (2005). Trends, prospects and challenges in quantifying flow and transport through fractured rocks. *Hydrogeology Journal*, 13(1), 124-147. doi:10.1007/s10040-004-0397-2
- Novakowski, K. (1992). The Analysis of Tracer Experiments Conducted in Divergent Radial Flow Fields. *Water Resources Research*, 28(12), 3215-3225.
- O'Melia, C. (1980). Aquasols: the behavior of small particles in aquatic systems. *Environmental Science & Technology*, 14(9), 1052-1060.
- Passmore, J. M., Rudolph, D. L., Mesquita, M. M. F., Cey, E. E., & Emelko, M. B. (2010). The utility of microspheres as surrogates for the transport of E. coli RS2g in partially saturated agricultural soil. *Water Research*, 44(4), 1235-45. doi:10.1016/j.watres.2009.10.010
- Piggot, A. R., & Elsworth, D. (1993). Laboratory Assessment of the Equivalent Apertures of a Rock Fracture. *Geophysical Research Letters*, 20(13), 1387-90.
- Powelson, D. K., Simpson, J. R., & Gerba, C. P. (1991). Effects of organic matter on virus transport in unsaturated flow. *Applied and Environmental Microbiology*, 57(8), 2192-2196.
- Pyrak-Nolte, L. J., Cook, N. G. W., & Nolte, D. D. (1987). Fluid Percolation through Single Fractures. *Geophysical Research Letters*, 15(11), 1247-1250.
- Rasmuson, A., & Neretnieks, I. (1986). Radionuclide Transport in Fast Channels in Crystalline Rock. *Water Resources Research*, 22(8), 1247. doi:10.1029/WR022i008p01247

- Raven, K., & Gale, J. (1985). Water Flow in a Natural Rock Fracture as a Function of Stress and Sample Size. *International Journal of Rock Mechanics and Mining Sciences & Geomechanics Abstracts*, 22(4), 251-261.
- Reimus, P. W. (1995). The Use of Synthetic Colloids in Tracer Transport Experiments in Saturated Rock Fractures. *Report LA-13004-T, Los Alamos National Laboratory, Los Alamos, NM*, (Vol. 18). Retrieved from <http://www.ncbi.nlm.nih.gov/pubmed/21904770>
- Reitsma, S., & Kueper, B. H. (1994). Laboratory measurement of capillary pressure saturation curves in a natural rock fracture. *Water Resources Research*, 30(4), 865-878.
- Schmidt, Philip J, Emelko, M. B., & Reilly, P. M. (2010). Quantification of analytical recovery in particle and microorganism enumeration methods. *Environmental Science & Technology*, 44(5), 1705-1712. doi:10.1021/es902237f
- Shapiro, A. M., & Hsieh, P. A. (1998). How Good are Estimates of Transmissivity from Slug Tests in Fractured Rock? *Ground Water*, 36(1), 37-48.
- Sharma, M. M., Chamoun, H., Sita Rama Sarma, D. S. H., & Schecter, R. S. (1992). Factors Controlling the Hydrodynamic Detachment of Particles from Surfaces. *Journal of Colloid and Interface Science*, 149(1), 121-134.
- Taylor, R., Cronin, A., Pedley, S., Barker, J., & Atkinson, T. (2004). The implications of groundwater velocity variations on microbial transport and wellhead protection - review of field evidence. *FEMS Microbiology Ecology*, 49(1), 17-26. doi:10.1016/j.femsec.2004.02.018
- Torkzaban, S., Bradford, S. A., & Walker, S. L. (2007). Resolving the Coupled Effects of Hydrodynamics and DLVO Forces on Colloid Attachment in Porous Media. *Langmuir*, (17), 9652-9660. doi:10.1029/2005WR004851.(11)
- Wood, W. W., Kraemer, T. F., & Shapiro, A. M. (2004). Radon (²²²Rn) in ground water of fractured rocks: A diffusion/ion exchange model. *Ground Water*, 42, 552-567.
- Zhao, Z., Jing, L., & Neretnieks, I. (2010). Evaluation of hydrodynamic dispersion parameters in fractured rocks, 2(3), 243-254. doi:10.3724/SP.J.1235.2010.00243
- Zheng, Q., Dickson, S. E., & Guo, Y. (2008). On the appropriate equivalent aperture for the description of solute transport in single fractures : Laboratory-scale experiments. *Water Resources Research*, 44(4) 1-9. American Geophysical Union. Retrieved from <http://cat.inist.fr/?aModele=afficheN&cpsidt=20346527>
- Zheng, Q., Dickson, S. E., & Guo, Y. (2009). Differential transport and dispersion of colloids relative to solutes in single fractures. *Journal of colloid and interface science*, 339(1), 140-151. doi:10.1016/j.jcis.2009.07.002
- Zimmerman, R. W., & Bodvarsson, G. (1996). Hydraulic Conductivity of Rock Fractures. *Transport in Porous Media*, 23(1), 1-30.

Zimmerman, R. W., & Yeo, I. W. (2000). Fluid Flow in Rock Fractures: From the Navier-Stokes Equations to the Cubic Law. *Dynamics of Fluids in Fractures Rocks*, 122, 213-224.

Appendix

Appendix A: Bromide Tracer Tests

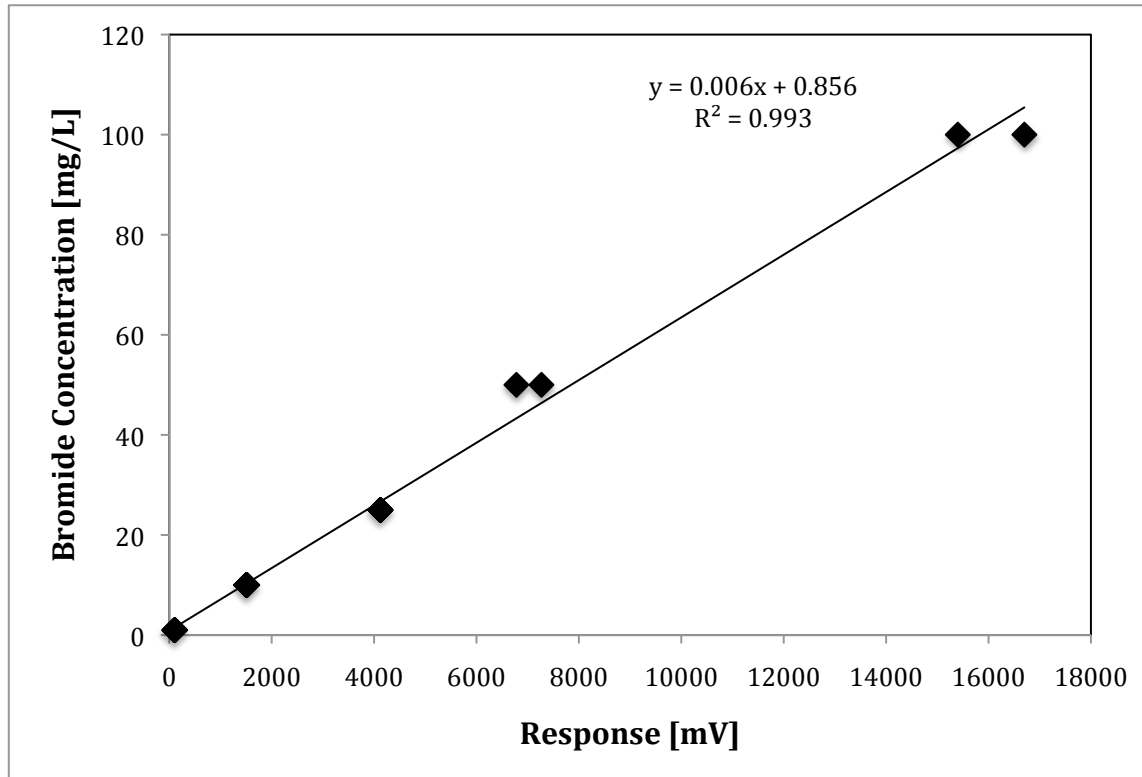


Figure A-1: Solute tracer test HPLC standards response curve for F1 at $q=30\text{m/d}$.

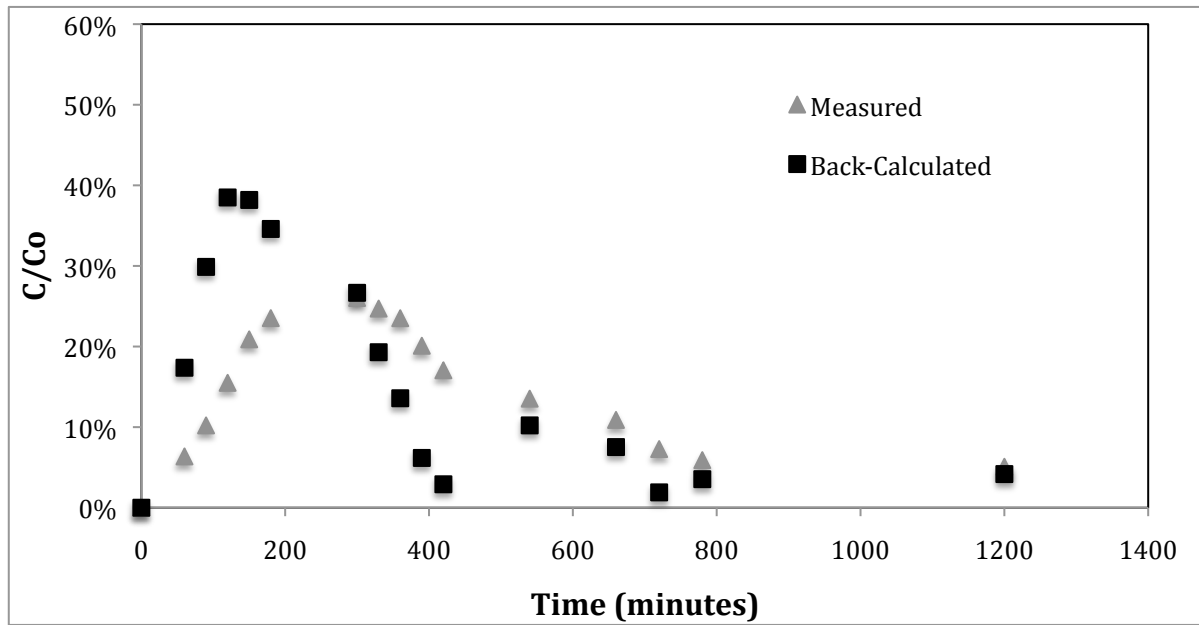


Figure A-2a: F1, $q=30$ m/d

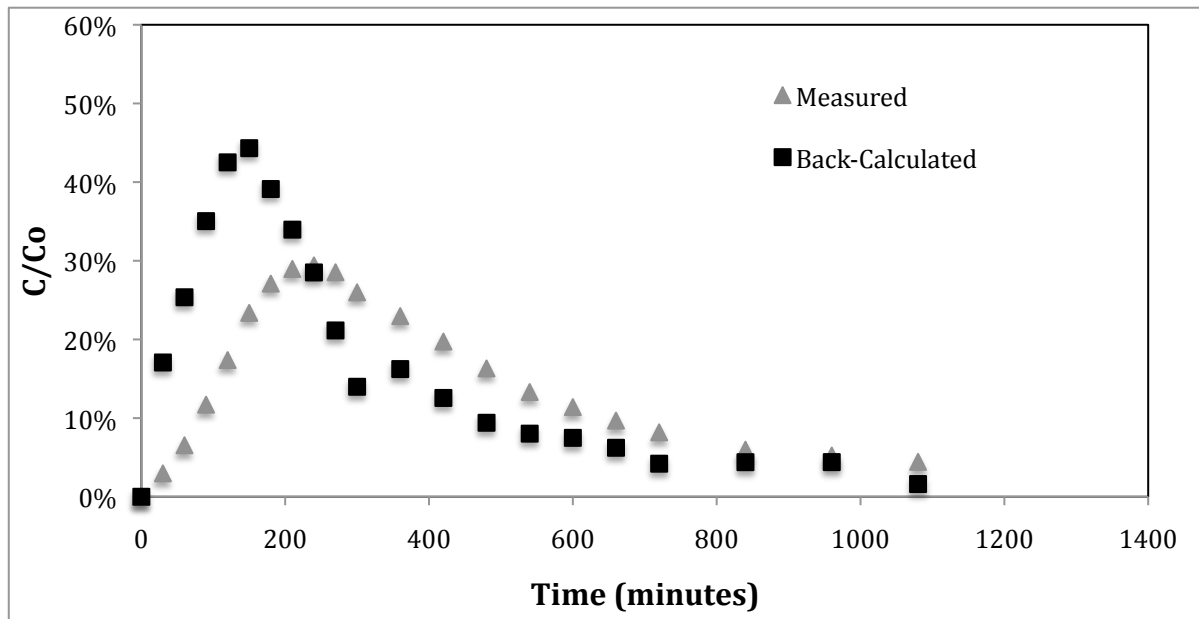


Figure A-2b: F1, $q=30$ m/d (duplicate)

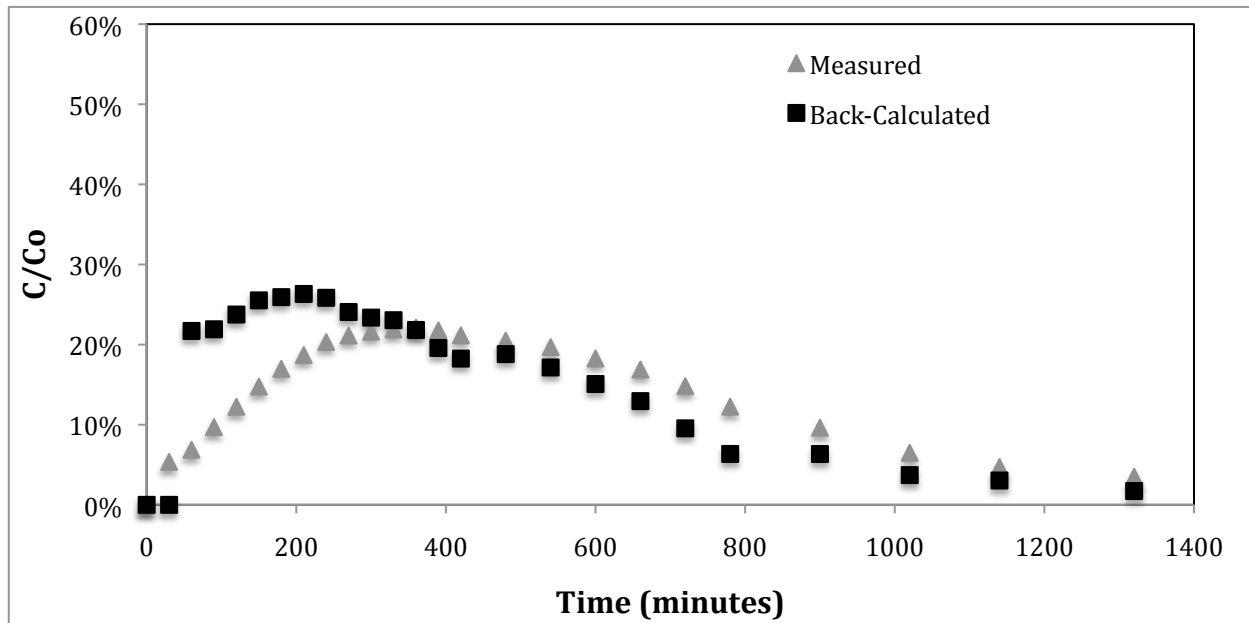


Figure A-2c: F2, $q=30$ m/d

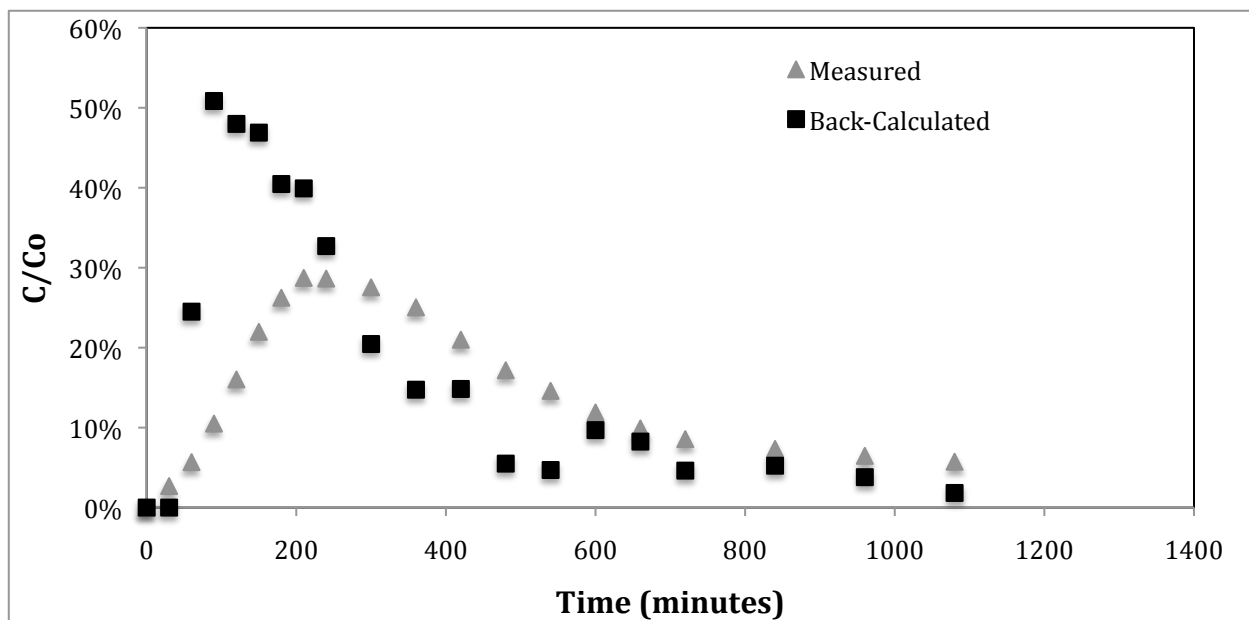


Figure A-2d: F2, $q=30$ m/d (duplicate)

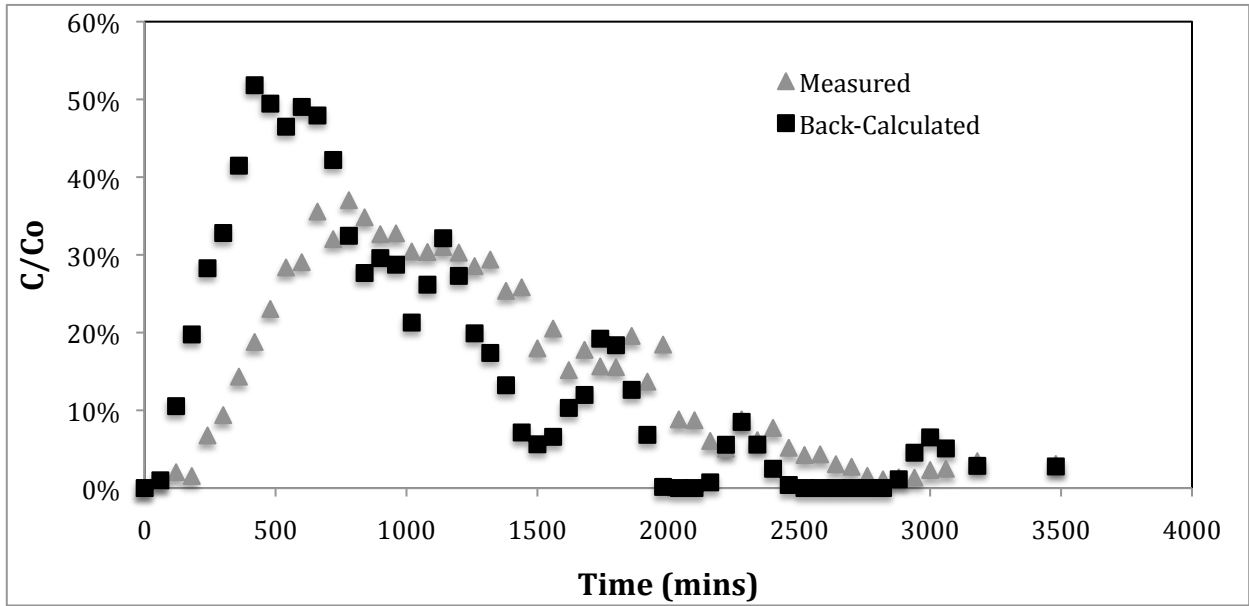


Figure A-2e: F1, $q=10$ m/d

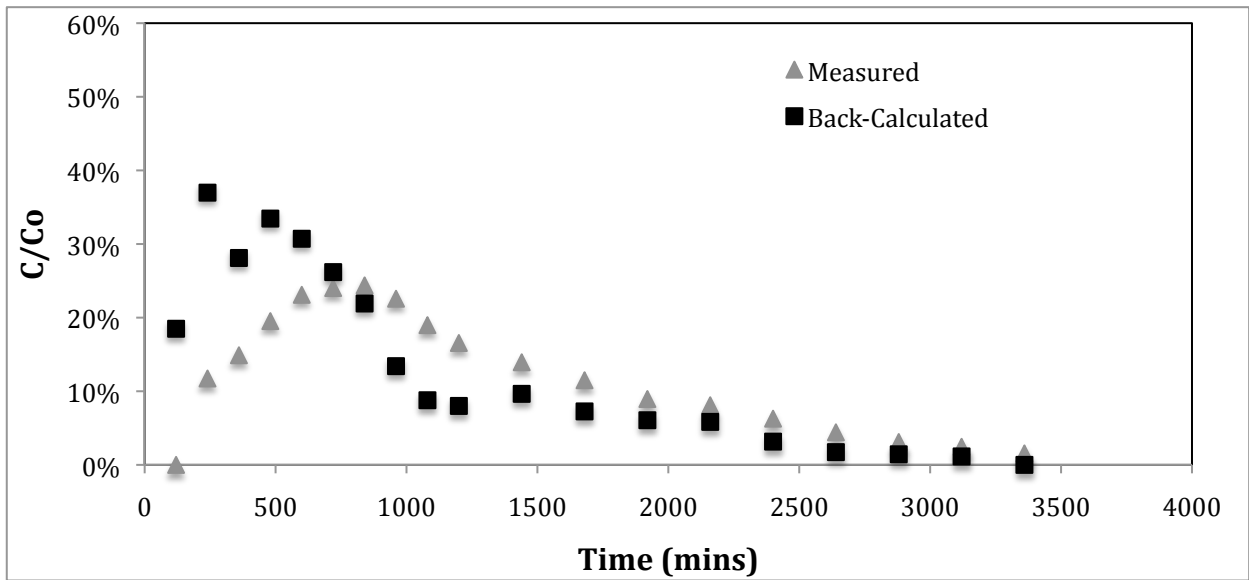


Figure A-2f: F2, $q=10$ m/d

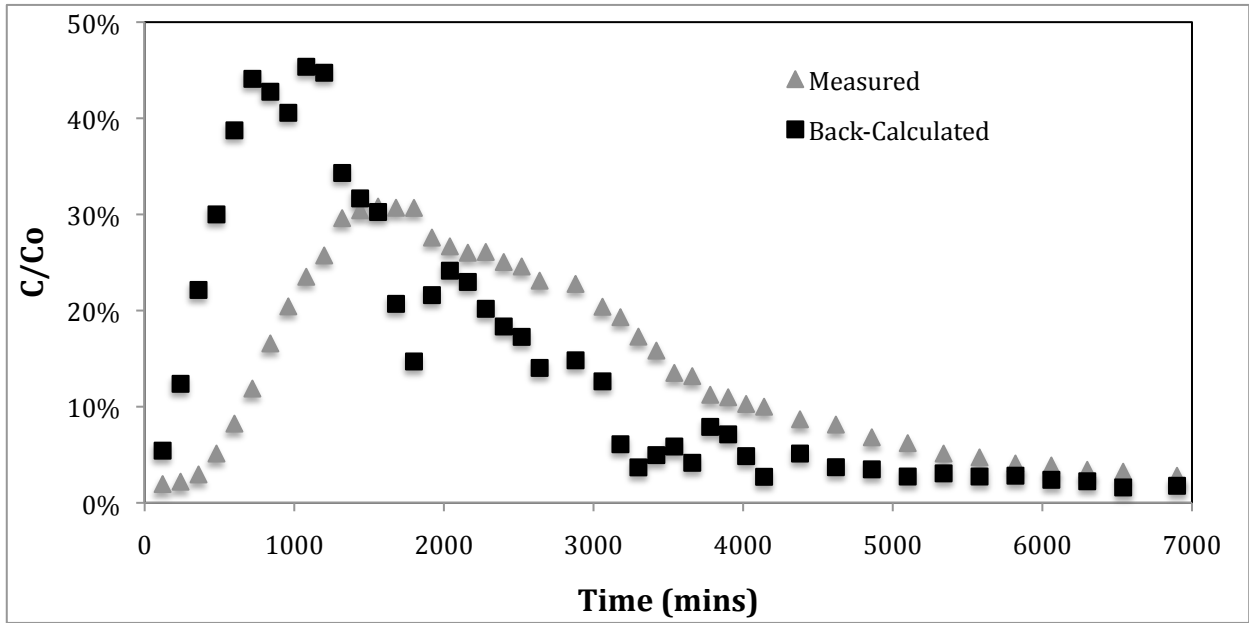


Figure A-2g: F1, $q=5$ m/d

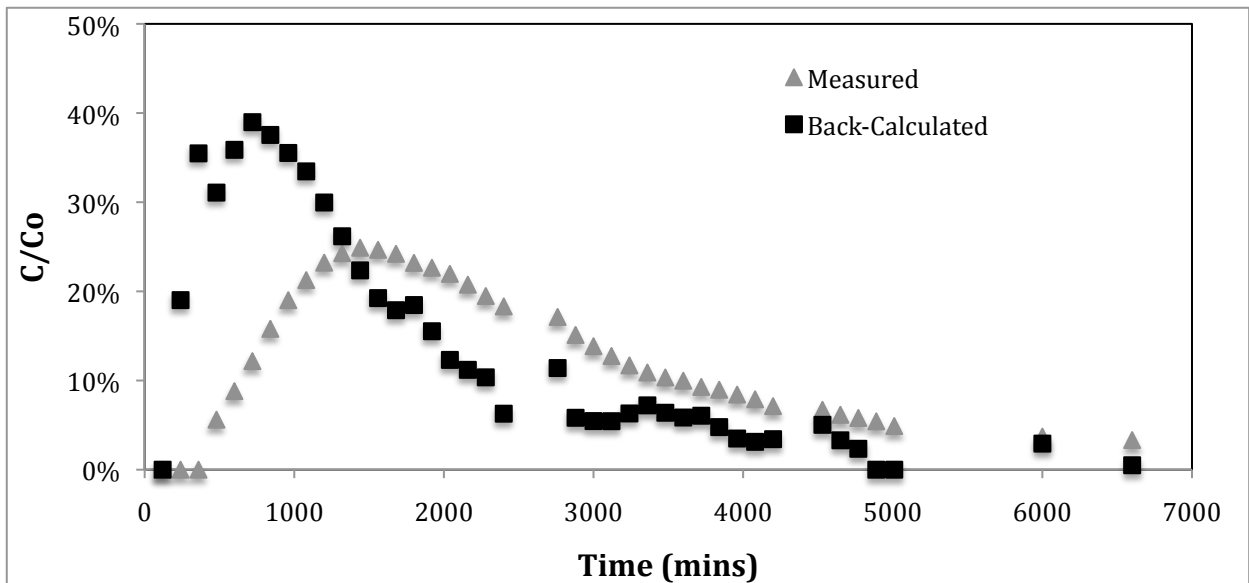


Figure A-2h: F2, $q=5$ m/d

Appendix B: *E. coli* RS2GFP Tracer Tests

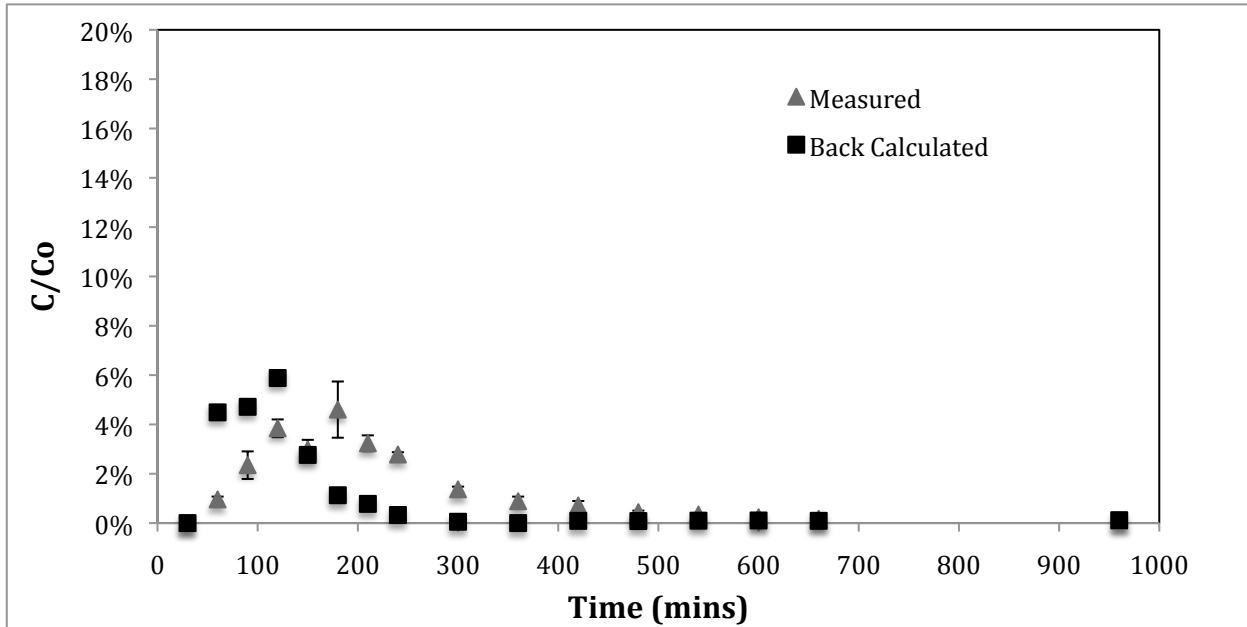


Figure B-1a: F1, q=30m/d

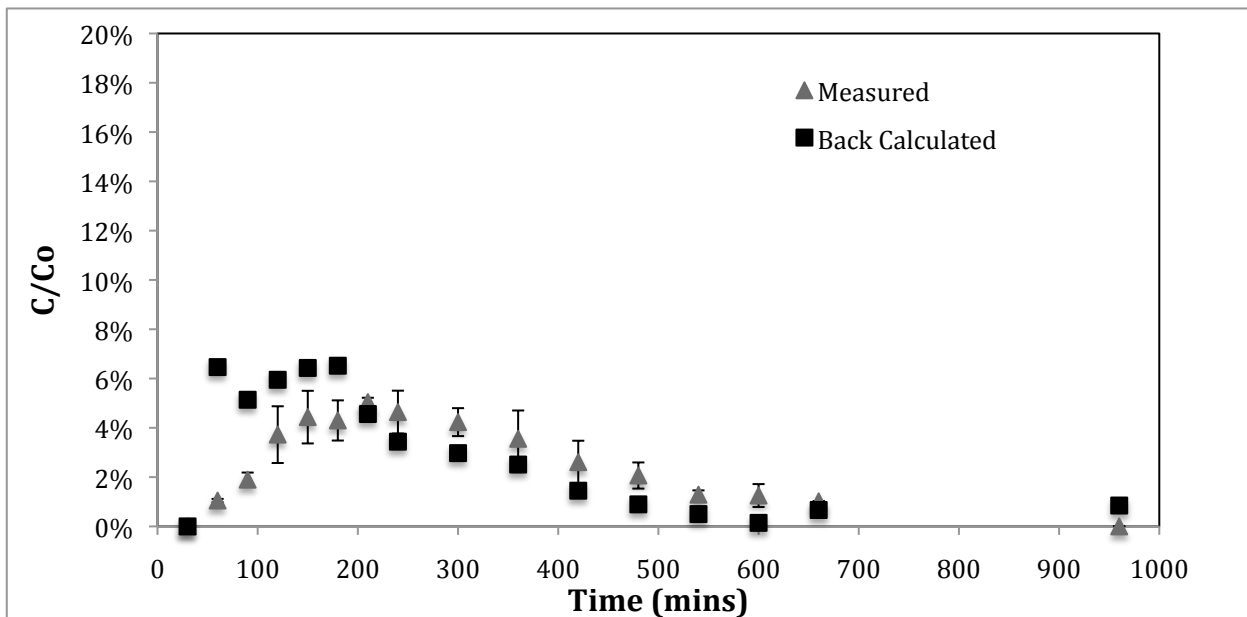


Figure B-1b: F1, q=30m/d (duplicate)

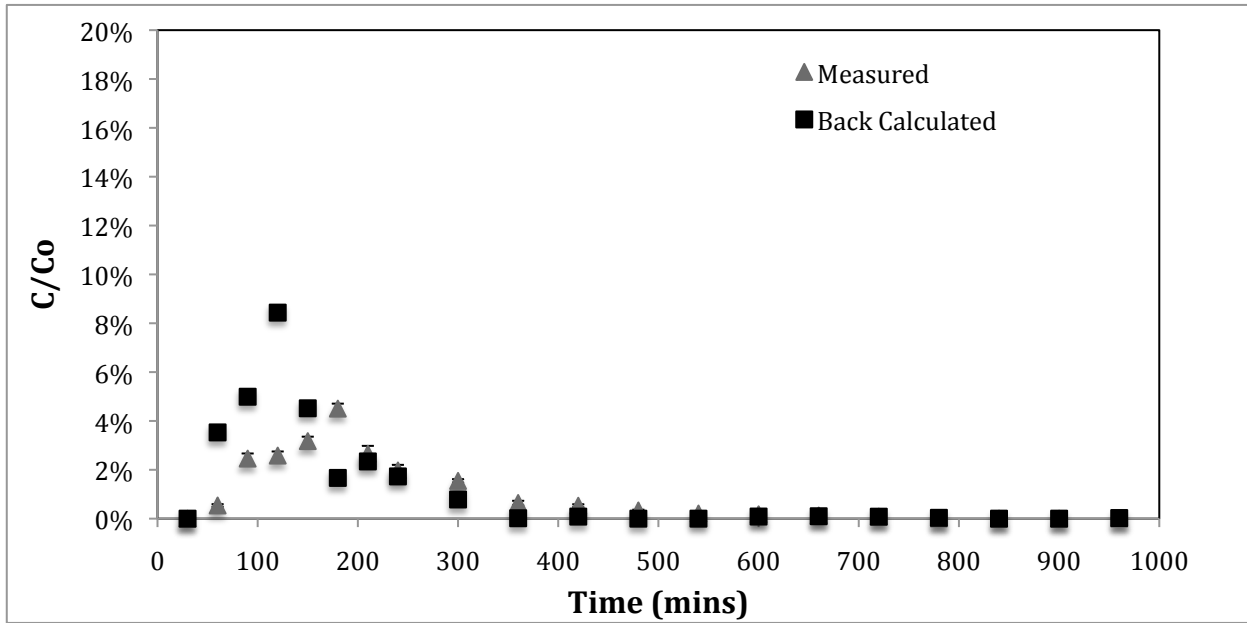


Figure B-1c: F2, q=30m/d

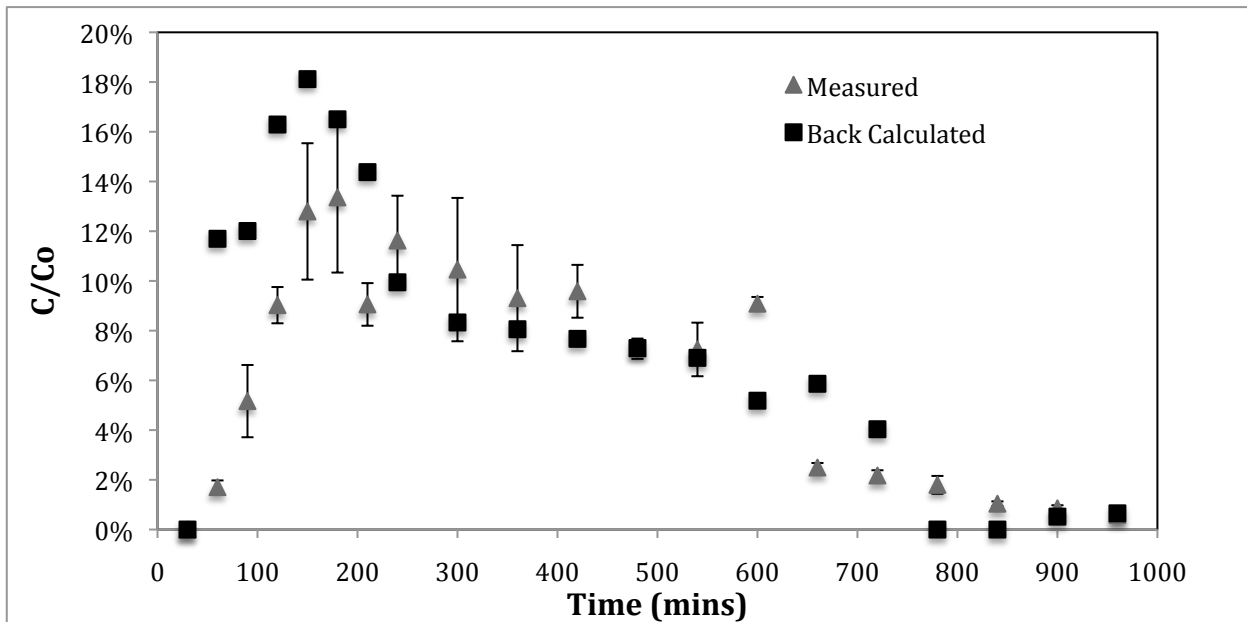


Figure B-1d: F2, q=30m/d (duplicate)

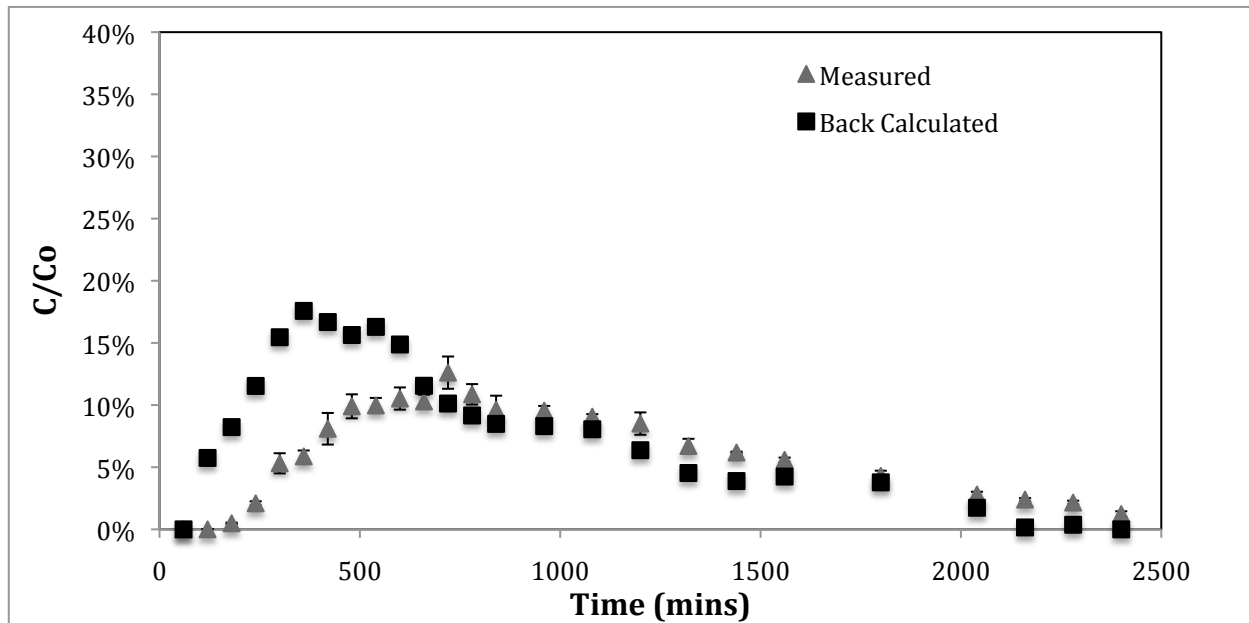


Figure B-1e: F1, $q=10$ m/d

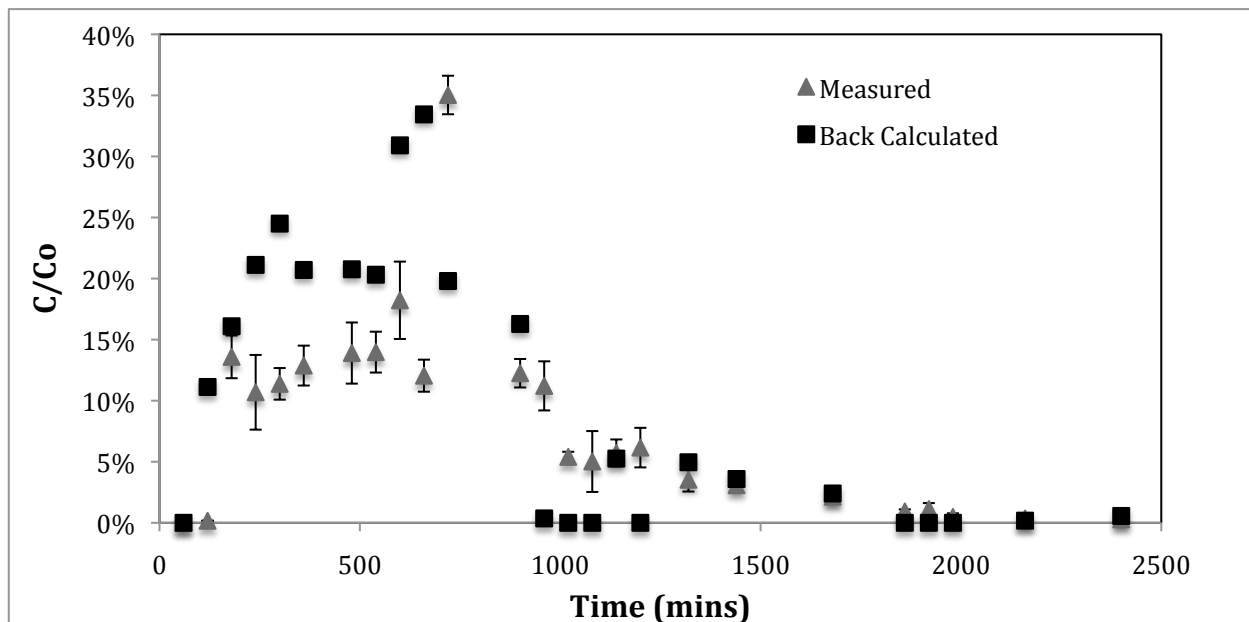


Figure B-1f: F2, $q=10$ m/d

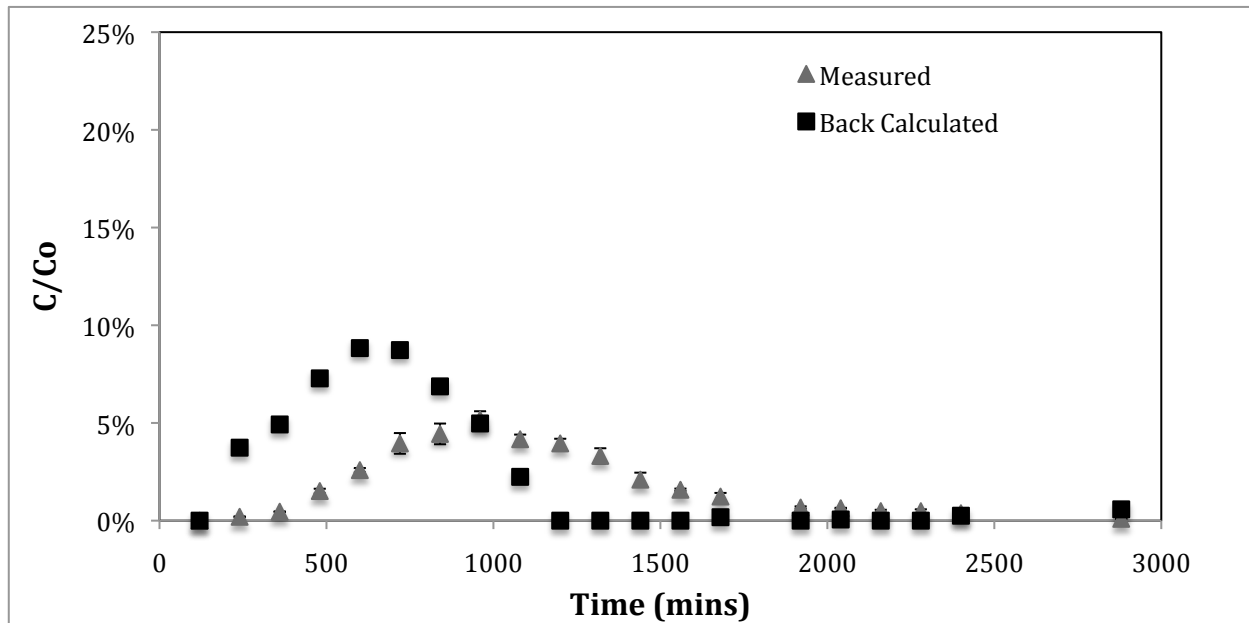


Figure B-1g: F1, 5 m/d

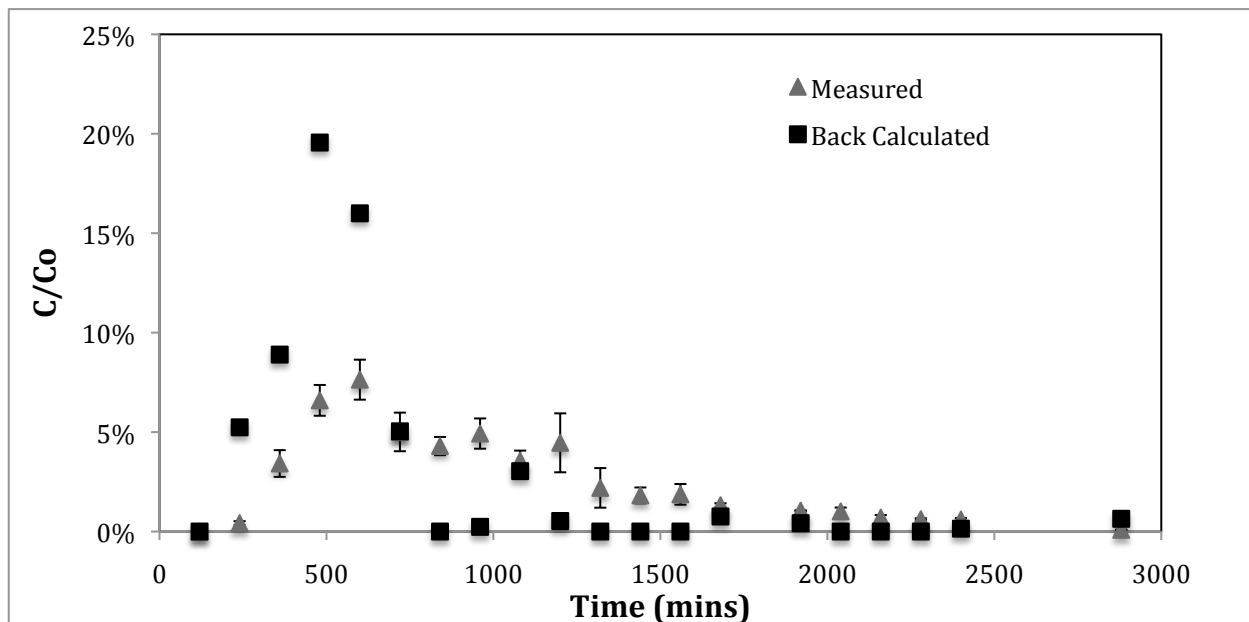


Figure B-1h: F2, 5m/d

Appendix C: Microsphere Tracer Tests

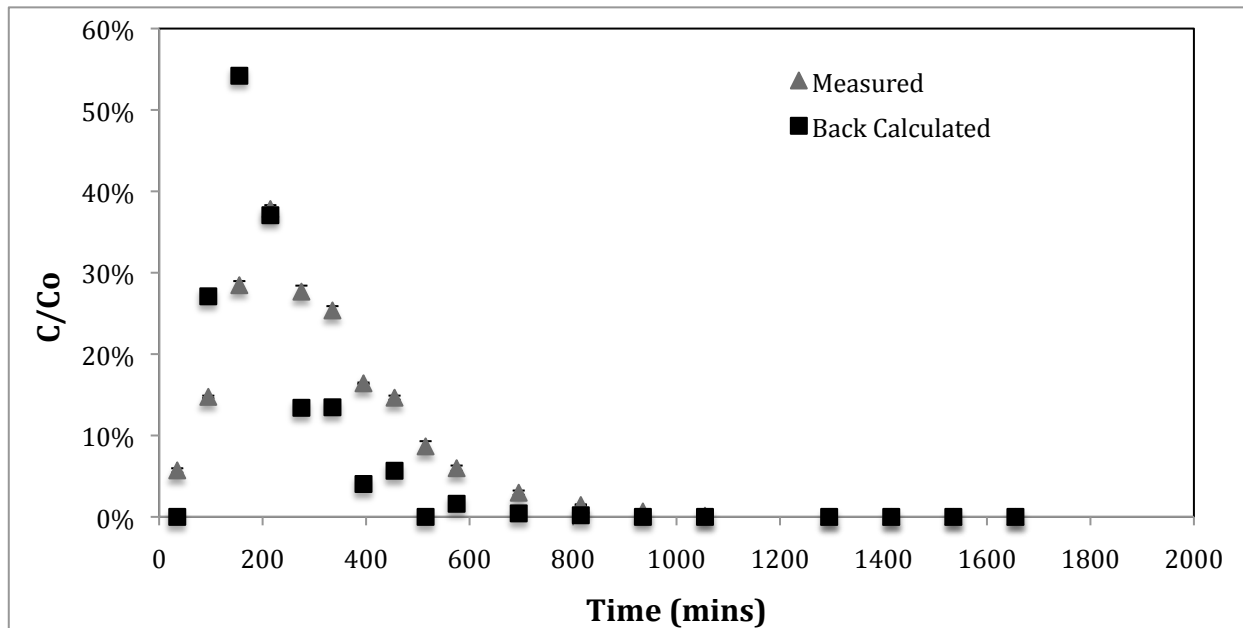


Figure C-1a: F1, $q=30$ m/d

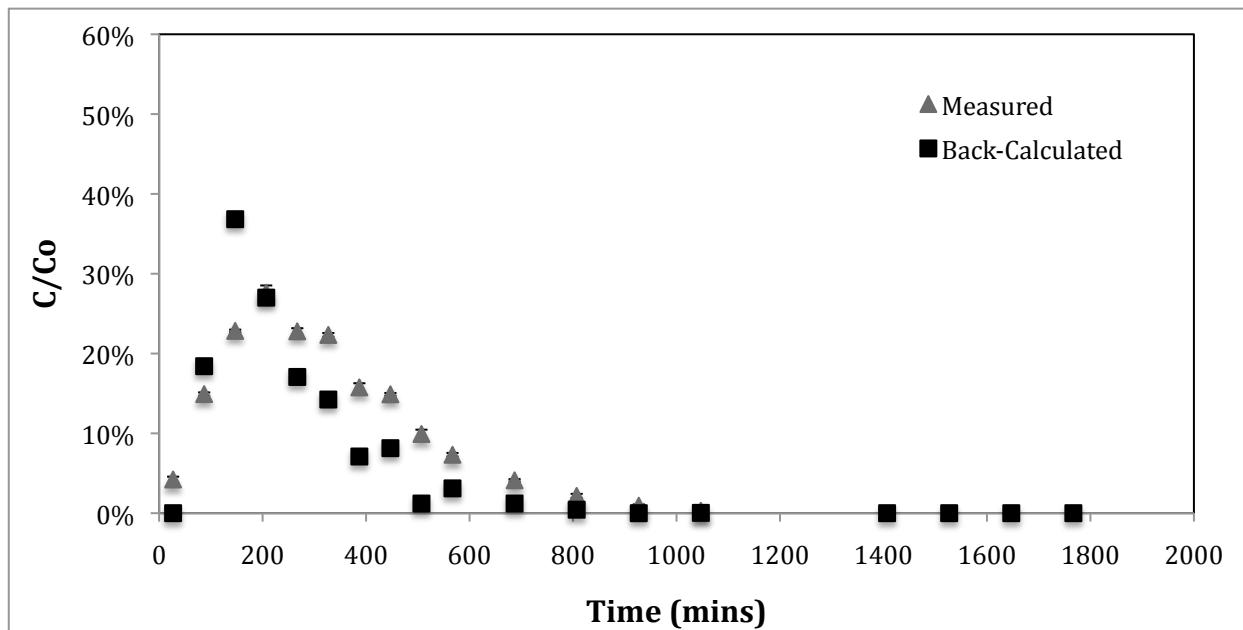


Figure C-1b: F2, $q=30$ m/d

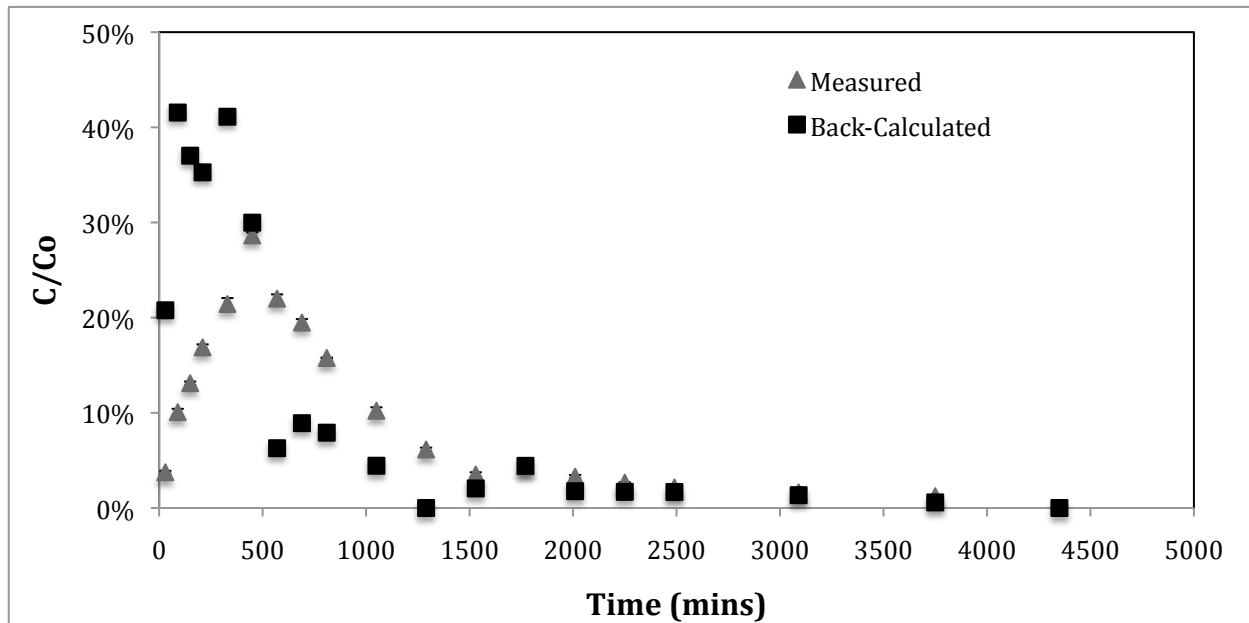


Figure C-1c: F2, q=10 m/d

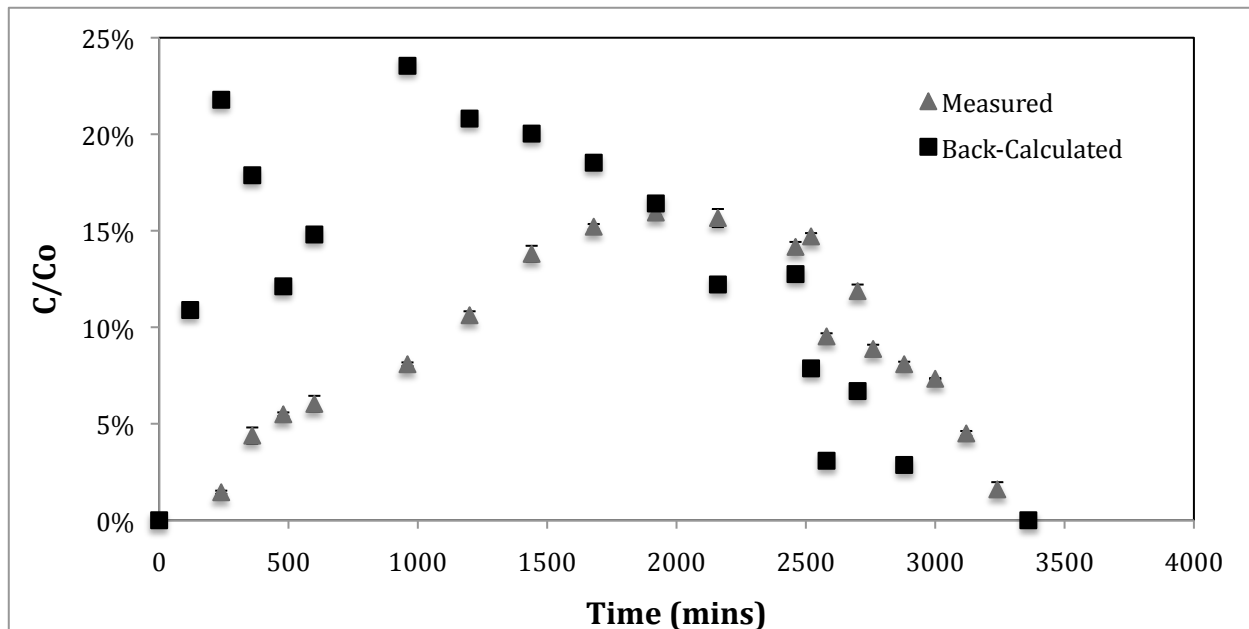


Figure C-1d: F2, q=5 m/d